RhTrx-1 ameliorates miroglial neuroinflammation after cerebral ischemic stroke

Yang Jiao
Second affiliated hospital of Harbin Medical University
Jianjian Wang
Second hospital of Harbin Medical University
Huixue Zhang
The second affiliated hospital of Harbin Medical Hospital
Yuze Cao
Peking Union Medical College Hospital
Yang Qu
Harbin Medical University
Siyu Huang
Harbin Medical University
Xiaotong Kong
The second affiliated hospital of Harbin Medical University
Chang Song
The second affiliated hospital of Harbin Medical University
Jie Li
The second affiliated hospital of Harbin Medical University
Qian Li
The second affiliated hospital of Hrbin Medical University
Heping Ma
Emory University School of Medicine
Xiaoyu Lu
Second affiliated hospital of Harbin Medical University
Lihua Wang (✉ wanglh211@163.com)
The Second Affiliated Hospital of Harbin Medical University

Research

Keywords: Ischemic stroke, Microglia, Neuroinflammation, RIPK1, rhTrx-1

Posted Date: March 20th, 2020

DOI: https://doi.org/10.21203/rs.3.rs-18172/v1

Abstract

Background

Microglia are rapidly activated after ischemic stroke and participate in the occurrence of neuroinflammation, which exacerbates the injury of ischemic stroke. Receptor Interacting Serine Threonine Kinase 1 (RIPK1) is thought to be involved in the development of inflammatory responses, but its role in ischemic microglia remains unclear. Here, we applied recombinant human thioredoxin-1 (rhTrx-1), a potential neuroprotective agent, to explore the role of rhTrx-1 in inhibiting RIPK1-mediated neuroinflammatory responses in microglia.

Method

Middle cerebral artery occlusion (MCAO) and Oxygen and glucose deprivation (OGD) were conducted for in vivo and in vitro experimental stroke models. The expression of RIPK1 in microglia after ischemia was examined. The inflammatory response of microglia was analyzed after treatment with rhTrx-1 and Necrostatin-1 (Nec-1, inhibitors of RIPK1), and the mechanisms were explored. In addition, the effects of rhTrx-1 on neurobehavioral deficits and cerebral infarct volume were examined.

Results

RIPK1 expression was detected in microglia after ischemia. Molecular docking results showed that rhTrx-1 could directly bind to RIPK1. In vitro experiments found that rhTrx-1 reduced necroptosis, mitochondrial membrane potential damage, Reactive oxygen species (ROS) accumulation and NLR Family, pyrin domain-containing 3 protein (NLRP3) inflammasome activation by inhibiting RIPK-1 expression, and regulated microglial M1/M2 phenotypic changes, thereby reducing the release of inflammatory factors. Consistently, in vivo experiments found that rhTrx-1 treatment attenuated cerebral ischemic injury by inhibiting the inflammatory response.

Conclusion

Our study demonstrates the role of RIPK1 in microglia-arranged neuroinflammation after cerebral ischemia. Administration of rhTrx-1 provides neuroprotection in ischemic stroke-induced microglial neuroinflammation by inhibiting RIPK1 expression.

Background

The global incidence of ischemic stroke has been increasing year by year, becoming the leading cause of disability and death of adults worldwide [1]. Within minutes to hours after the onset of acute ischemic stroke, the rapid occurrence of neuroinflammation response mediates the damage of brain tissue and cells after ischemia, thus becoming an important cause of acute ischemic injury [2, 3]. Microglia is the important immunocompetent cell in the central nervous system [4]. After the occurrence of ischemic stroke, it rapidly activates into different phenotypes, and then participates in the damage or repair of

ischemic brain tissue by regulating the occurrence of neuroinflammatory reactions [5, 6]. The molecular mechanisms that regulate microglial activation are still unclear. Exploring the mechanism is beneficial to the development of effective drugs for the treatment of cerebral ischemic injury [7, 8].

RIPK1 plays an important role in mediating inflammatory response [9]. RIPK1 can initiate necroptosis by activating RIPK3, which then induces necrosis-like changes in cells and releases inflammatory factors [10]. In addition to relying on the necroptosis pathway to release inflammatory factors, RIPK1 can also release inflammatory factors by driving NLRP3 inflammasome [11]. Compared with the therapeutic effect of inhibiting apoptosis, intracerebroventricular injections of Nec-1 (a specific inhibitor of RIPK1) could reduce the volume of cerebral infarction more effectively at an earlier time [12, 13]. It implies that treatment with targeted inhibition of RIPK1 conducive to widen the time window of treatment in the acute phase of cerebral infarction. Current studies suggested that neurons undergoing necroptosis could recruit microglia leading to secondary injury by releasing inflammatory factors [14]. However, the role of RIPK1 in driving the inflammatory response in microglia after cerebral ischemia is still unclear. Therefore, further exploration is needed.

Inhibiting the inflammatory response after acute phase reperfusion play an important role for the treatment of cerebral infarction [2, 3, 15]. Thioredoxin-1 (Trx-1) is a small molecule hydrogen donor widely present in cells and has a variety of biological functions, such as antioxidant and anti-inflammatory [16, 17]. Studies have found that overexpression of Trx-1 provides effective neuroprotective effects on the brain tissue of MCAO mice, while inhibition of Trx-1 exacerbates the neuroinflammatory response in MCAO mice [18–20]. These findings provide a strong scientific basis for the clinical translational application of Trx-1. RhTrx-1 is a compound extracted and synthesized from Escherichia coli. Current studies have shown that using rhTrx-1 treatment could reduce cerebral infarction volume and improve neurological deficits in MCAO mice. Besides, rhTrx-1 treatment could alleviate ischemia-induced neuron injury [21–23]. However, the protective and regulatory effects of rhTrx-1 on microglia after cerebral ischemia remain unclear. On these bases, our study aims to investigate the therapeutic potential of rhTrx-1 in inhibiting RIPK1-driven neuroinflammation in microglia after cerebral ischemia.

Methods

Chemical Materials

Pentobarbital sodium was safeguarded in Harbin Medical Pharmacological Laboratory (Harbin, China). BSA and rhTrx-1 were purchased from R&D System (St. Paul, Minnesota, USA). Penicillin/streptomycin solution, Hoechst and 2% TTC dyeing solution were purchased from Solarbio (Beijing, China). ROS and Necrostatin-1 was purchased from Sigma (St. Louis, MO, USA). Annexin V-PE/7AAD assay was purchased from BD Biosciences (San Jose, CA, USA). All the ELISA kits were purchased from Cusabio (Wuhan, China). Dapi dyeing solution and JC-1 kit were purchased from Beyotime (Shanghai, Beijing). DMEM, FBS amd MEM/EBSS were purchased from Hyclone (Logan, Utah, USA). The primary antibodies used were: anti-RIPK1, anti-RIPK3, anti-MLKL, anti-pMLKL, anti-CCL2 and anti-Iba-1 (Abcam, Cambridge,

MA, USA); another anti-Iba-1 (Wako, Japan); anti-NLRP3, anti-ASC, anti-caspase-1, anti-caspase-3 and anti-β-actin (ABclonal, Wuhan, China); anti-CD206 and anti-MMP-9 (R&D System, St. Paul, Minnesota, USA); anti-CD16 (Bioss, Beijing, China). The second antibodies used were: Alexa Fluor 800-conjugated Goat-anti rabbit (LI-COR, Lincoln, NE, USA), Alexa Fluor 555-conjugated Donkey-anti Rabbit, Alexa Fluor 488-conjugated Donkey-anti Rabbit, Alexa Fluor 488-conjugated Donkey-anti Goat (Abcam, Cambridge, MA, USA).

MCAO Procedure And Drug Administration

C57 BL/6 male mice received 60 min of MCAO as previous described with some modifications [24]. Briefly, thirty-eight mice were randomly divided into three groups: Sham, MCAO and MCAO + rhTrx-1 group. All mice were anesthetized with pentobarbital sodium before inducing MCAO. During the operation, mice body temperature was kept at 37℃. For MCAO procedure, common carotid artery (CCA), external carotid artery (ECA) and internal carotid artery (ICA) were exposed and separated. After clipping the common carotid artery, ligation was performed at the ECA and a small incision was made. Through the incision, thread embolism was slowly inserted into ICA. After 60 min occlusion, thread embolism was pulled out and the reperfusion was carried out. Mice in Sham group received the same procedure, but did not receive the embolus. The mice in MCAO + rhTrx-1 group received 10 mg/kg rhTrx-1 by tail vein injection after reperfusion. As control, mice in MCAO group were injected with equal volume of 0.9% sterile saline. All mice were sacrificed 24 h after reperfusion for further analysis.

Infarct Volume Assessment

TTC staining was executed to evaluate the size of cerebral infarction. In brief, the brain was taken to make coronal brain sections after the mice were sacrificed. The slices were placed in 2% TTC staining solution and immersed for 10 min at 37℃ avoiding meeting up. After staining, the slices were fixed in 4% PFA overnight, and pictured the next day. Each infarct area was measured by using Image J software.

Neurobehavioral Testing

To assess the degree of sensory and motor damage in each group of mice, Bederson score and corner test were carried out based on previous studies [25, 26]. In order to evaluate Bederson score, scores were recorded according to the physical signs of the mice in the tail suspension state as followed: 0 points, normal; 1 point, the contralateral forelimb could not be fully extended; 2 points, the resistance to thrust of the contralateral forelimb decreased; 3 points, turning to the contralateral side of the lesion. For evaluation corner test, mice were placed in the depth of 30-degree angle, and the direction of turning was observed. Normal mice turned randomly and with equal probability toward both sides, whereas mice turned toward the lesion side after cerebral ischemia.

OGD Procedure And Treatment

BV-2 cell line were cultured in complete medium, and incubated in 37℃ incubator containing 5% CO_2. The complete medium was composed of DMEM containing 10% Fetal Bovine Serum (FBS) and 1%

penicillin/streptomycin solution. For the OGD program, after replacing the cell supernatant with EBSS solution, the cells were transferred to three gas incubators (37℃, containing 95% N_2 and 5% CO_2) and cultured for 1, 2, or 4 h, respectively. Cells in the Nec-1 group were treated with Nec-1 (20 μM) after re-oxygenation and maintained for 6 h, 12 h, 24 h. Cells in the rhTrx-1 group were incubated with 5, 10 or 25 μg/ml rhTrx-1 (dissolved in sterile PBS) for 24 h after reoxygenation.

Flow Cytometry

To detect apoptotic rate and intracellular ROS expression level, Annexin V-PE/7AAD kit and DCFH-DA solution were used according to the manufacturer's instructions. Briefly, to analyze the extent of apoptosis, cells were harvested and double-stained with Annexin V-PE and 7AAD for 15 min at room temperature in the dark. To detect intracellular ROS levels, cells were harvested and stained with DCFH-DA solution for 20 min in the dark at 37℃. Immediately after the above staining, the cells were detected and analyzed using a Beckman CytoFLEX flow cytometer (CA, USA).

Western Blot Analysis

The protein levels were detected by western blot. In a brief, cells or brain tissues were lysed in precooled RIPA buffer and centrifuged to collect the supernatant for protein extraction. Samples were loaded onto SDS-PAGE and then transferred onto nitrocellulose membranes. Membranes were blocked with 5% BSA or 5% non-fat dry milk and finally incubated with primary antibodies (anti-RIPK1, anti-RIPK3, anti-MLKL, anti-pMLKL, anti-CCL2, anti-MMP-9, anti-NLRP3, anti-ASC, anti-caspase-1, anti-caspase-3 and anti-β-actin) at 4℃ overnight. The second day membranes were incubated with Alexa Fluor 800-conjugated Goat-anti rabbit antibody at room temperature. Protein bands were imaged and analyzed with the Odyssey system (LI-COR Biosciences, Lincoln NE, USA).

Transmission Electron Microscope (TEM)

After collecting the cell precipitation, glutaraldehyde was added slowly for fixation. Ultrathin cell sections (100 nm thick) prepared using ultramicrotome were mounted on a copper grid, and then stained with uranyl acetate and lead citrate. Observed the sections at an accelerating voltage of 80 kV on a transmission electron microscope (Hitachi H-7100, Hitachinaka, Japan) by single blind.

Immunofluorescence Staining

Briefly, for in vitro test, cells were fixed with 4% paraformaldehyde (PFA) for 15 min and then washed with PBS for 3 times and then incubated with first antibodies. After incubated with the anti-CD206 or anti-CD16 primary antibody respectively at 4℃ overnight, cells were incubated with the secondary antibodies at room temperature for 1 h, and were added Hoechst finally. For in vivo test, frozen slices were only washed with PBS for 3 times and then blocked with 5% BSA at room temperature for 1 h. The anti-RIPK1, anti-CD206, anti-CD16 and Iba-1 primary antibody were incubated respectively. The Alexa Fluor 555-conjugated Donkey-anti Rabbit, Alexa Fluor 488-conjugated Donkey-anti Rabbit, Alexa Fluor 488-

conjugated Donkey-anti Goat second antibodies were used finally. The slices and cells were imaged with fluorescence microscopy (ZEISS, Jena, Germany). The whole scan were imaged with Leica image scope (Leica, Heidelberg, Germany) .

ROS Detection

Before collecting cells, DCFH-DA was diluted with serum-free DMEM at a dilution ratio of 1:1000. To detect the intracellular generation of ROS in vitro, treated cells were incubated with diluted DCFH-DA solution for 20 min in a 37℃ incubator protected from light. After washed three times with serum-free cell culture medium, cells were immediately acquired under a fluorescence microscope (ZEISS) and analyzed by using Image J software.

Mitochondrial Membrane Potential (MMP) Assay

JC-1 staining kit was used to measure the MMP in vitro according to instructions. Briefly, JC-1 buffer solution and working solution was prepared after the cells subjected to 4 h OGD and 24 h reoxygenation. The appropriate volume of JC-1 working solution was added to fully cover the cells instead of cell culture medium, and then cultured the cells in 37℃ incubator for 20 min. After washing 3 times with JC-1 buffer solution, cells were examined immediately under ZEISS fluorescence microscope.

ELISA

To detect the inflammatory factor levels, cell supernatant or brain tissues were collected and ELISA were performed according to the instructions. Briefly, 50 μL sample and 100 μL antibody being tested were added to the reaction wells respectively and then placed the wells-plate in a 37℃ incubator and incubated for 60 min in the dark. After incubation with termination solution, the OD value was measured at 450 to measure the expression levels of TNF-α, IL-1β and TGF-β.

Molecular Docking

The structures of rhTrx-1 and RIPK1 were processed and optimized using Accelrys Discovery Studio 2016 platform (San Diego, CA, USA), and protein docking was performed and calculated in ZDOCK module. Poses with the best scores were selected and then further energy optimization was performed using the RDock program. The interaction between rhTrx-1 and RIPK1 was analyzed using the Analyze Protein Interface module. Finally, Pymol (DeLano Scientific. Palo Alto, CA, USA) was used for mapping.

Statistical Analysis

GraphPad Prism (Version 6.0c) software was used for statistics. Student's T test and One-factor Analysis of Variance (One-Way ANOVA) were used to evaluate the statistical significance. The results were presented using mean standard deviation. $P < 0.05$ was considered statistically significant.

Results

RIPK1 was induced in the microglia of MCAO following reperfusion

We applied the MCAO model and examined the expression of RIPK1 in the mouse brain 24 h after reperfusion. Firstly, we removed samples from the contralateral hemisphere and the ipsilateral hemisphere, and then examined samples by using western blot. As described in Fig. 1a and 1b, expression of RIPK1 was significantly increased on the ipsilateral hemisphere compared with the contralateral hemisphere. Next, to assess the localization of RIPK1 in microglia, the double staining of RIPK1 and Iba-1 was examined by the whole scan analysis. We found that RIPK1 exhibited in microglia of MCAO (Fig. 1c, d). These results indicated that RIPK1 was induced in the microglia of MCAO following reperfusion.

RIPK1-induced Necroptosis Protein Levels Of OGD Microglia In Vitro

To investigate the degree of microglial necroptosis at different OGD time, flow cytometry was performed. The results showed that the number of early apoptotic and late apoptotic microglia gradually increased with the prolongation of OGD time (Fig. 2a) and was the highest at 24 h of reoxygenation after 4 h of GOD (Fig. 2b). Based on this, further investigation of RIPK1 level at different reoxygenation time after 4 h of GOD presented that RIPK1 peaked at 6 h of reoxygenation (Fig. 2c). Furthermore, therapeutic treatment of Nec-1 restrained RIPK1, RIPK3, and pMLKL/MLKL levels compared with untreated groups (Fig. 2d, e). The inhibitory effect was most significant at 24 h of reoxygenation. Taken together, these results indicated that necroptosis was augmented in microglia following ischemia reperfusion.

RhTrx-1 decreased RIPK1-induced necroptosis and apoptosis of OGD microglia in vitro

To characterize the role of rhTrx-1, we computerized the binding interaction of rhTrx-1 and RIPK1. Docking analysis illustrated that total six Pi interactions, five Hydrogen Bonds and one Salt Bridges were exhibited between rhTrx-1 and RIPK1 (Table S1), which indicated rhTrx1 directly binds with RIPK1 (Fig. 3a, b). Further detection showed 5 μg/mL, 10 μg/mL and 25 μg/mL dose of rhtTx-1 treatment inhibited the expression of RIPK1, RIPK3, and pMLKL/MLKL after 4 h of OGD, and the inhibitory effect of rhTrx-1 was more obvious in the dose of 25 μg/mL (Fig. 3c, d). According to these, follow-up experiments were carried out with 25 μg/mL concentration as the rhTrx-1 action concentration. Subsequent investigation revealed that rhTrx-1 and Nec-1 treatment reduced Cleaved-Caspase-3 level (Fig. 3e). Ultrastructural images of TEM showed cell structures of OGD-induced microglia in rhTrx-1 and Nec-1 treatment groups were more similar to the control group (Fig. 3f). In addition, compared to the untreated groups, fewer microglia underwent early and late apoptosis in rhTrx-1 and Nec-1 treatment group after OGD (Fig. 3g, h).

Therapeutic treatment with rhTrx-1 mitigated OGD-induced microglia mitochondrial injury and NLRP3 inflammasome activation

To determine the impact of rhTrx-1 on the mitochondrial injury in ischemia microglia, we measured the mitochondrial potential by using JC-1 staining. The mitochondrial membrane potential was dwindled (aggregate was decreased and monomer increased) after OGD 4 h/reoxygenation 24 h, whereas rhTrx-1

and Nec-1 treatment reversed the reduction of potential (Fig. 4a, b). Further detection proved that rhTrx-1 and Nec-1 treatment eliminated the accumulation of ROS in OGD-induced microglia (Fig. 4c, d). Lastly, inflammasome proteins levels were examined to determine the activation of inflammasome. Compared to untreated groups, NLRP3, ASC and Cleaved-Caspase-1 levels in rhTrx-1 and Nec-1 treatment groups were significance decreased (Fig. 4e, f), and the release of IL-1β was cleared simultaneous as well (Fig. 4g).

Therapeutic treatment with rhTrx-1 regulated OGD-induced microglia polarization and inhibited the release of inflammation mediators

To clarify the effect of rhTrx-1 on the microglia polarization, we observed the intensity of CD16 and CD206. As demonstrated in Fig. 5a, b, the fluorescence intensity of CD16, representing M1-type microglia, enhanced in OGD and significantly abated after treatment with rhTrx-1 and Nec-1. Contrast to this, the fluorescence intensity of M2 microglia-labeled CD206 was increased and treatment with rhTrx-1 and Nec-1 strengthened the augment (Fig. 5c, d). Moreover, the increased inflammation mediators CCL2, MMP-9, and TNF-α level were erased after rhTrx-1 and Nec-1 treatment, and the expression of TFG-β increased further compared to untreated group.

Administration Of rhTrx-1 Reduced Acute Cerebral Ischemic Stroke Injury

We examined the neurological function of mice after 24 h of MCAO reperfusion. Berderson score and corner test results showed that neurological deficits of rhTrx-1 treated MCAO mice were significantly reduced compared with untreated MCAO mice (Fig. 6a, b). The volume size of cerebral infarction was detected by TTC staining, and the size of cerebral infarction in the rhTrx-1 treatment group was significantly smaller than that in the untreated MCAO group (Fig. 6c). The results of TTC staining supported the results of neurobehavioral testing.

Administration of rhTrx-1 reduced RIPK1-mediated microglia inflammation factors release in MCAO mice

To verify the therapeutic effect of rhTrx-1 in vivo, we measured the RIPK1 level in rhTrx-1 treated MCAO mice. Identically, the expression of RIPK1 was uniformly inhibited by administration of rhTrx-1 (Fig. 7a, b). Next, the numbers of $CD16^+$/Iba-1^+ and $CD206^+$/Iba-1^+ positive microglia was counted to estimate the polarization of M1/M2-type microglia. Immunofluorescence staining results demonstrated that rhTrx-1 inhibited M1-type microglia activation and promoted M2-type microglia activation in vivo (Fig. 7c-f). Finally, ELISA results showed that rhTrx-1 administration significantly erased the release of inflammatory mediators TNF-α and IL-1β (Fig. 7g, h)

Discussion

The microglial neurotoxicity is directly related to the adverse outcome of ischemic brain injury [5, 6, 27, 28]. In this study, we performed MCAO and OGD procedure assessing RIPK1-mediated inflammatory

response in microglia, and found that rhTrx-1 can be used as an inhibitor of RIPK1 to regulate the inflammatory activation of microglia after cerebral ischemia.

RIPK1 is considered to be a key regulator of innate immunity, which can regulate the occurrence of inflammatory response [9]. Study has shown that mice lacking RIPK1 gene die of systemic multiple organ inflammation at birth [29]. As a promoter of programmed cell death, RIPK1 can recruit RIPK3 to form necrosome and finally activate the phosphorylation of MLKL to activate the necroptosis-signaling pathway. And therefore causes the cells to undergo necrotic changes and release pro-inflammatory mediators such as MMP-9 and TNF-α to intensify the neuroinflammation [30, 31]. Huang and Fan et al proved that Nec-1 could inhibit the inflammatory response mediated by microglia in the retina and spinal cord by activating necroptosis pathway [32, 33]. These suggest that treatment of inhibiting necroptosis pathway in microglia may be beneficial to provide anti-inflammatory effects for ischemic stroke. In our data, we showed that RIPK1 level increased after MCAO, and found that RIPK1 localized in microglia. To figure out its role in ischemic stroke-induced microglial neuroinflammation, we detected the expression level of RIPK1 in vitro. We found that the expression of RIPK1 increased with the prolong of reoxygenation time in microglia. In the context of Nec-1 or rhTrx-1 treatment, the induction of necroptosis by RIPK1 was significantly decreased in OGD-induced microglia indicating that rhTrx-1 has similar pharmacological effects to Nec-1. In accordance with these results, we further used a docking model and found that rhTrx-1 directly binds to RIPK1 with Pi interactions, salt bridge and hydrogen bonds. It illustrated that rhTrx-1 can be directly combined with RIPK1 and produced a marked effect in the inhibition of RIPK1.

In addition to activating necroptosis, RIPK1 can initiate apoptosis as a scaffold protein [34]. Although it is believed that apoptosis does not involve in the release of inflammatory factors, the apoptotic microglia may indirectly aggravate the damage of cerebral ischemic tissues and cells due to the loss of normal physiological functions. We found that rhTrx-1 and Nec-1 treatment reduced the activation of cleave-caspase-3 after OGD in microglia, suggesting rhTrx-1 has anti-apoptotic effect in ischemic microglia by inhibiting RIPK1 level. Besides, RIPK1 can activate the expression of pyruvate dehydrogenase (PDH) complex by recruiting RIPK3, which promotes the release of ROS accumulation in mitochondria. And that make further efforts to increase the expression of ROS in a feed forward manner [35, 36]. In this way, that kind of loop promotes the accumulation of ROS, leading to mitochondrial damage and activation of mitochondrial-mediated apoptosis [37]. When we studied the expression of ROS in microglia and the change of mitochondrial membrane potential, we found that rhTrx-1 effectively inhibited the pathological accumulation of ROS and rescued mitochondrial injury. Such protective effect might be due to the inhibition of the cascade reaction of RIPK1. Of course, rhTrx-1 has antioxidant effect on its own biological characteristics, which affects mitochondrial function and ROS release by affecting cell oxidative respiratory chain during treatment [38]. However, due to the complexity of oxidative stress injury mechanism, the study of oxidative stress therapy cannot be single. At least, our study provides evidence for the therapeutic effect of rhTrx-1 from another perspective.

It has been reported that the activation of RIPK3-MLKL can directly trigger the activation of NLRP3 inflammasome in renal tubular cells [39]. Furthermore, RIPK1 can trigger the activation of NLRP3 inflammasome by destroying mitochondria membrane and promoting the release of ROS, which further promotes the production and secretion of IL-1β to extracellular and initiate neuroinflammation. To investigate the role of rhTrx-1 in RIPK1-induced NLRP3 inflammasome activation, we examined the levels of NLRP3, ASC and cleaved-caspase-1 and indicated that rhTrx-1 ultimately reduced the release of IL-1β, depending on the inhibition of NLRP3 inflammasome. These results highlight the role of rhTrx-1 in inhibiting microglia associated-inflammation in cerebral ischemic stroke.

Compared with MCAO group, rhTrx-1 treatment alleviated the absence of neurological deficit after MCAO, and effectively inhibited the volume of cerebral infarction. Similar to our results, Hattori et al found that rhTrx-1 was able to permeate the blood-brain barrier and significantly ameliorated neurological function deficit and infarct volume size [21]. Ma et al investigated that rhTrx-1 exerts an antioxidative and antinitrative effect against neurological dysfunction and cerebral infarction [22]. On these basis, we further considered the activation of microglia in vitro and in vivo. The activated microglia after ischemia details a dual function of promoting inflammation and anti-inflammation due to its polarization to M1/M2 phenotype conversion [6, 40, 41]. We found that rhTrx-1 treatment increased M2 phenotype microglia and decreased M1 phenotype after OGD procedure. Consistently, we also observed that rhTrx-1 treatment predisposed the microglia phenotype to M2 type in the in vivo MCAO model. Moreover, we showed that TGF-β released by microglia was increased, while the release of TNF-α, CCL2 and MMP-9 were decreased compared with the untreated group. These data provides evidences for rhTrx-1 inhibiting inflammation mediated by RIPK1. The results also prove from the side that inhibiting the expression of RIPK1 can make microglia gradually show its original advantages in repairing brain tissue damage and promoting angiogenesis.

Conclusions

In conclusion, our study found that RIPK1 plays an important role in microglia-mediated neuroinflammatory response after cerebral ischemia. It can regulate the conversion of microglia M1/M2 phenotype, reduce the release of inflammatory factors and ultimately reduce the occurrence of neuroinflammation by inhibiting necroptosis and activation of NLRP3 inflammasome. RhTrx-1 can act as a RIPK1 inhibitor to provide neuroprotection in microglial inflammation induced by inhibiting RIPK1 expression in ischemic stroke.

Abbreviations

ASC: Apoptosis-associated speck-like protein containing CARD; CCL2: Chemokine (C-C motif) Ligand 2; CD16: Clusters of Differentiation 16; CD206: Clusters of Differentiation 206; DMEM: Dulbecco Modified Eagle Medium; EBSS: Earle's Balanced Salt Solution; Iba-1: Ionized calcium binding adaptor molecule-1; IL-1β: Interleukin-1β; MCAO: Middle cerebral artery occlusion; MLKL: Mixed Lineage Kinase Domain-like Protein; MMP-9: Matrix metalloproteinase-9; Nec-1: Necrostatin-1; NLRP3: NLR Family, pyrin domain-

containing 3 protein; OGD: Oxygen and glucose deprivation; rhTrx-1: Recombinant human thioredoxin-1; RIPK1: Receptor Interacting Serine Threonine Kinase 1; RIPK3: Receptor Interacting Serine Threonine Kinase 3; ROS: Reactive oxygen species; TEM: Transmission Electron Microscope; TGF-β: Transforming Growth Factor-β; TNF-α: Tumor Necrosis Factor-α; Trx: Thioredoxin; TTC: 2,3,5-triphenyltetrazolium chloride.

Declarations

Ethics approval and consent to participate

All experiments were conducted in accordance with the guidelines published by Harbin Medical University Ethics committee.

Consent for publication

Not applicable.

Availability of data and materials

The datasets used and/or analyzed during the current study are available from the corresponding author on reasonable request.

Competing interests

The authors declare that they have no competing interests

Funding

This work was supported by National Key Research and Development Project (2018YFE0114400), National Natural Science Foundation of China (grant nos. 81820108014, 81771361, 81701155, 81801190 and 81901277).

Authors' contributions

YJ designed the study, participated in all experiments, and coordinated all stages of manuscript preparation. JJW, HUZ and YZC helped conceive the study. YQ and SYH assisted in the implementation of the experiments. XTK and CS helped draft the manuscript. JL and QL participated in data analysis. LHW, XYL and HPM reviewed all stages of the study. All authors agreed to submit the final manuscript to the Journal of Neuroinflammation.

Acknowledgements

Not applicable.

References

1. Wang W, Jiang B, Sun H, Ru X, Sun D, Wang L, Wang L, Jiang Y, Li Y, Wang Y, Chen Z, Wu S, Zhang Y, Wang D. Prevalence, Incidence, and Mortality of Stroke in China: Results from a Nationwide Population-Based Survey of 480 687 Adults. Circulation. 2017;135(8):759-771.
2. Jayaraj RL, Azimullah S, Beiram R, Jalal FY, Rosenberg GA. Neuroinflammation: friend and foe for ischemic stroke. J Neuroinflammation. 2019;16(1):142.
3. Mo Y, Sun YY, Liu KY. Autophagy and inflammation in ischemic stroke.Neural Regen Res. 2020;15:1388-1396.
4. Ayata P, Schaefer A. Innate sensing of mechanical properties of brain tissue by microglia. Curr Opin Immunol. 2020;62:123-130.
5. Rupalla K 1, Allegrini PR, Sauer D, Wiessner C. Time course of microglia activation and apoptosis in various brain regions after permanent focal cerebral ischemia in mice. Acta Neuropathol. 1998;96(2):172-178.
6. Feng Y, He X, Luo S, Chen X, Long S, Liang F, Shi T, Pei Z, Li Z. Chronic colitis induces meninges traffic of gut-derived T cells, unbalances M1 and M2 microglia/macrophage and increases ischemic brain injury in mice. Brain Res. 2019;1707:8-17.
7. Wang R, Pu H, Ye Q, Jiang M, Chen J, Zhao J, Li S, Liu Y, Hu X, Rocha M, Jadhav AP, Chen J, Shi Y. Transforming Growth Factor Beta-Activated Kinase 1-Dependent Microglial and Macrophage Responses Aggravate Long-Term Outcomes After Ischemic Stroke. Stroke. 2020;51(3):975-985.
8. Lu YM, Huang JY, Wang H, Lou XF, Liao MH, Hong LJ, Tao RR, Ahmed MM, Shan CL, Wang XL, Fukunaga K, Du YZ. Targeted therapy of brain ischaemia using Fas ligand antibody conjugated PEG-lipid nanoparticles. Biomaterials. 2014;35:530-537.
9. Muscolino E, Schmitz R, Loroch S, Caragliano E, Schneider C, Rizzato M, Kim YH, Krause E, Juranić Lisnić V. Herpesviruses induce aggregation and selective autophagy of host signalling proteins NEMO and RIPK1 as an immune-evasion mechanism. Nat Microbiol. 2020;5:331-342.
10. Chen S, Lv X, Hu B, Shao Z, Wang B, Ma K, Lin H, Cui M. RIPK1/ RIPK3/ MLKL-mediated necroptosis contributes to compression-induced rat nucleus pulposus cells death. Apoptosis. 2017;22:626-638.
11. Wang X, Jiang W, Yan Y, Gong T, Han J, Tian Z, Zhou R. RNA viruses promote activation of the NLRP3 inflammasome through a RIP1-RIP3-DRP1 signaling pathway. Nat Immunol. 2014;15:1126-1133.
12. Deng XX, Li SS, Sun FY. Necrostatin-1 Prevents Necroptosis in Brains after Ischemic Stroke via Inhibition of RIPK1-Mediated RIPK3/MLKL Signaling. Aging Dis. 2019;10:807-817.
13. Degterev A, Huang Z, Boyce M, Li Y, Jagtap P, Mizushima N, Cuny GD, Mitchison TJ, Moskowitz MA, Yuan J. Chemical inhibitor of nonapoptotic cell death with therapeutic potential for ischemic brain injury. Nat Chem Biol. 2005;1:112-119.
14. Yang J, Zhao Y, Zhang L, Fan H, Qi C, Zhang K, Liu X, Fei L, Chen S, Wang M, Kuang F, Wang Y, Wu S. RIPK3/MLKL-Mediated Neuronal Necroptosis Modulates the M1/M2 Polarization of Microglia/Macrophages in the Ischemic Cortex. Cereb Cortex. 2018;28:2622-2635.

15. Villapol S, Faivre V, Joshi P, Moretti R, Besson VC, Charriaut-Marlangue C. Early Sex Differences in the Immune-Inflammatory Responses to Neonatal Ischemic Stroke. Int J Mol Sci. 2019 Aug 4. doi: 10.3390/ijms20153809.
16. Gellert M, Hossain MF, Berens FJF, Bruhn LW, Urbainsky C, Liebscher V, Lillig CH. Substrate specificity of thioredoxins and glutaredoxins - towards a functional classification. Heliyon. 2019;5(12):e02943.
17. Holubiec MI, Galeano P, Romero JI, Hanschmann EM, Lillig CH, Capani F. Thioredoxin 1 Plays a Protective Role in Retinas Exposed to Perinatal Hypoxia-Ischemia. Neuroscience. 2020;425:235-250.
18. Zhou F, Gomi M, Fujimoto M, Hayase M, Marumo T, Masutani H, Yodoi J, Hashimoto N, Nozaki K, Takagi Y. Attenuation of neuronal degeneration in thioredoxin-1 overexpressing mice after mild focal ischemia. Brain Res. 2009;1272:62-70.
19. Takagi Y, Mitsui A, Nishiyama A, Nozaki K, Sono H, Gon Y, Hashimoto N, Yodoi J. Overexpression of thioredoxin in transgenic mice attenuates focal ischemic brain damage. Proc Natl Acad Sci U S A. 1999;96:4131-4136.
20. Li L, Zhu K, Liu Y, Wu X, Wu J, Zhao Y, Zhao J. Targeting thioredoxin-1 with siRNA exacerbates oxidative stress injury after cerebral ischemia/reperfusion in rats. Neuroscience. 2015;284:815-823.
21. Hattori I, Takagi Y, Nakamura H, Nozaki K, Bai J, Kondo N, Sugino T, Nishimura M, Hashimoto N, Yodoi J. Intravenous administration of thioredoxin decreases brain damage following transient focal cerebral ischemia in mice. Antioxid Redox Signal. 2004;6:81-87.
22. Ma YH, Su N, Chao XD, Zhang YQ, Zhang L, Han F, Luo P, Fei Z, Qu Y. Thioredoxin-1 attenuates post-ischemic neuronal apoptosis via reducing oxidative/nitrative stress. Neurochem Int. 2012;60:475-483.
23. Wang B, Tian S, Wang J, Han F, Zhao L, Wang R, Ning W, Chen W, Qu Y. Intraperitoneal administration of thioredoxin decreases brain damage from ischemic stroke. Brain Res. 2015;1615:89-97.
24. Chen Y, Zhang L, Ni J, Wang X, Cheng J, Li Y, Zhen X, Cao T, Jia J. LLDT-8 protects against cerebral ischemia/reperfusion injury by suppressing post-stroke inflammation. J Pharmacol Sci. 2016;131(2):131-137.
25. Bederson JB, Pitts LH, Tsuji M, Nishimura MC, Davis RL, Bartkowski H. Rat middle cerebral artery occlusion: evaluation of the model and development of a neurologic examination. Stroke. 1986;17:472-476.
26. Li X, Blizzard KK, Zeng Z, DeVries AC, Hurn PD, McCullough LD. Chronic behavioral testing after focal ischemia in the mouse: functional recovery and the effects of gender. Exp Neurol. 2004;187:94-104.
27. Lee JH, Wei ZZ, Cao W, Won S, Gu X, Winter M, Dix TA, Wei L, Yu SP. Regulation of therapeutic hypothermia on inflammatory cytokines, microglia polarization, migration and functional recovery after ischemic stroke in mice. Neurobiol Dis. 2016;96:248-260.
28. Sun W, Ding Z, Xu S, Su Z, Li H. Crosstalk between TLR2 and Sphk1 in microglia in the cerebral ischemia/reperfusion-induced inflammatory response. Int J Mol Med. 2017;40:1750-1758.
29. Rickard JA, O'Donnell JA, Evans JM, Lalaoui N, Poh AR, Rogers T, Vince JE, Lawlor KE, Ninnis RL, Anderton H. RIPK1 regulates RIPK3-MLKL-driven systemic inflammation and emergency

hematopoiesis. Cell. 2014;157:1175-1188.

30. Tang Q, Li W, Dai N, Gao Y, Han Y, Cheng G, Gu C. The Role of Necroptosis, Apoptosis, and Inflammation in Fowl Cholera-Associated Liver Injury in a Chicken Model. Avian Dis. 2017 Dec;61(4):491-502.
31. Radak D, Katsiki N, Resanovic I, Jovanovic A, Sudar-Milovanovic E, Zafirovic S, Mousad SA, Isenovic ER.Apoptosis and Acute Brain Ischemia in Ischemic Stroke. Curr Vasc Pharmacol. 2017;15:115-122.
32. Huang Z, Zhou T, Sun X, Zheng Y, Cheng B, Li M, Liu X, He C. Necroptosis in microglia contributes to neuroinflammation and retinal degeneration through TLR4 activation. Cell Death Differ. 2018;25:180-189.
33. Fan H, Zhang K, Shan L, Kuang F, Chen K, Zhu K, Ma H, Ju G, Wang YZ. Reactive astrocytes undergo M1 microglia/macrohpages-induced necroptosis in spinal cord injury. Mol Neurodegener. 2016;11:14.
34. Xu D, Jin T, Zhu H, Chen H, Ofengeim D, Zou C, Mifflin L, Pan L, Amin P, Li W, Shan B, Naito MG, Meng H. TBK1 Suppresses RIPK1-Driven Apoptosis and Inflammation during Development and in Aging. Cell. 2018;174:1477-1491.
35. Zhou JM, Gu SS, Mei WH, Zhou J, Wang ZZ, Xiao W. Ginkgolides and bilobalide protect BV2 microglia cells against OGD/reoxygenation injury by inhibiting TLR2/4 signaling pathways. Cell Stress Chaperones. 2016;21:1037-1053.
36. Yang Z, Wang Y, Zhang Y, He X, Zhong CQ, Ni H, Chen X, Liang Y, Wu J, Zhao S, Zhou D, Han J. RIP3 targets pyruvate dehydrogenase complex to increase aerobic respiration in TNF-induced necroptosis. Nat Cell Biol. 2018;20(2):186-197.
37. Andrabi SS, Parvez S, Tabassum H. Ischemic stroke and mitochondria: mechanisms and targets. Protoplasma. 2020;257(2):335-343.
38. Tan A, Nakamura H, Kondo N, Tanito M, Kwon YW, Ahsan MK, Matsui H, Narita M, Yodoi J. Thioredoxin-1 attenuates indomethacin-induced gastric mucosal injury in mice. Free Radic Res. 2007;41:861-869.
39. Chen H, Fang Y, Wu J, Chen H, Zou Z, Zhang X, Shao J, Xu Y. RIPK3-MLKL-mediated necroinflammation contributes to AKI progression to CKD. Cell Death Dis. 2018;9:87.
40. Zheng Y, He R, Wang P, Shi Y, Zhao L, Liang J. Exosomes from LPS-stimulated macrophages induce neuroprotection and functional improvement after ischemic stroke by modulating microglial polarization. Biomater Sci. 2019;7:2037-2049.
41. Ma Z, Zhang Z, Bai F, Jiang T, Yan C, Wang Q. Electroacupuncture Pretreatment Alleviates Cerebral Ischemic Injury Through α7 Nicotinic Acetylcholine Receptor-Mediated Phenotypic Conversion of Microglia. Front Cell Neurosci. 2019;13:537.

Figures

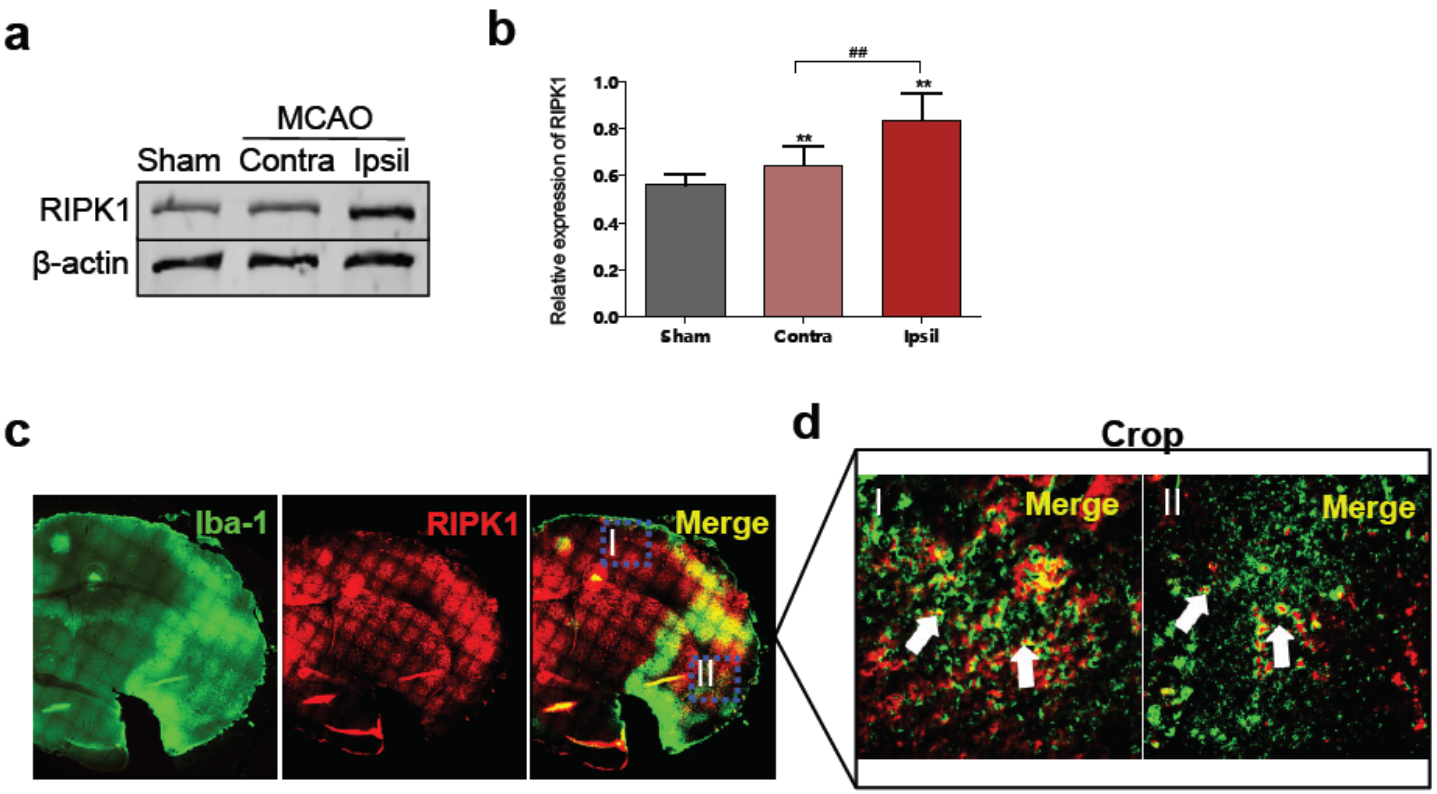

Figure 1

Detection of RIPK1 at 24 h following reperfusion in microglia of MCAO mice. a RIPK1 level was detected in the MCAO contralateral (Contra) hemisphere and ipsilateral (ipsil) hemisphere. b Quantification analysis of RIPK1 protein level. c Co-localization fluorescence staining of RIPK1 and microglia at 24 h following reperfusion by using whole scan. d Crop images from the merge image of the whole scan were showed. Scale bar represent 50 μm. **P<0.01 (vs Sham)##P < 0.01 (Contralateral vs Ipsilateral).

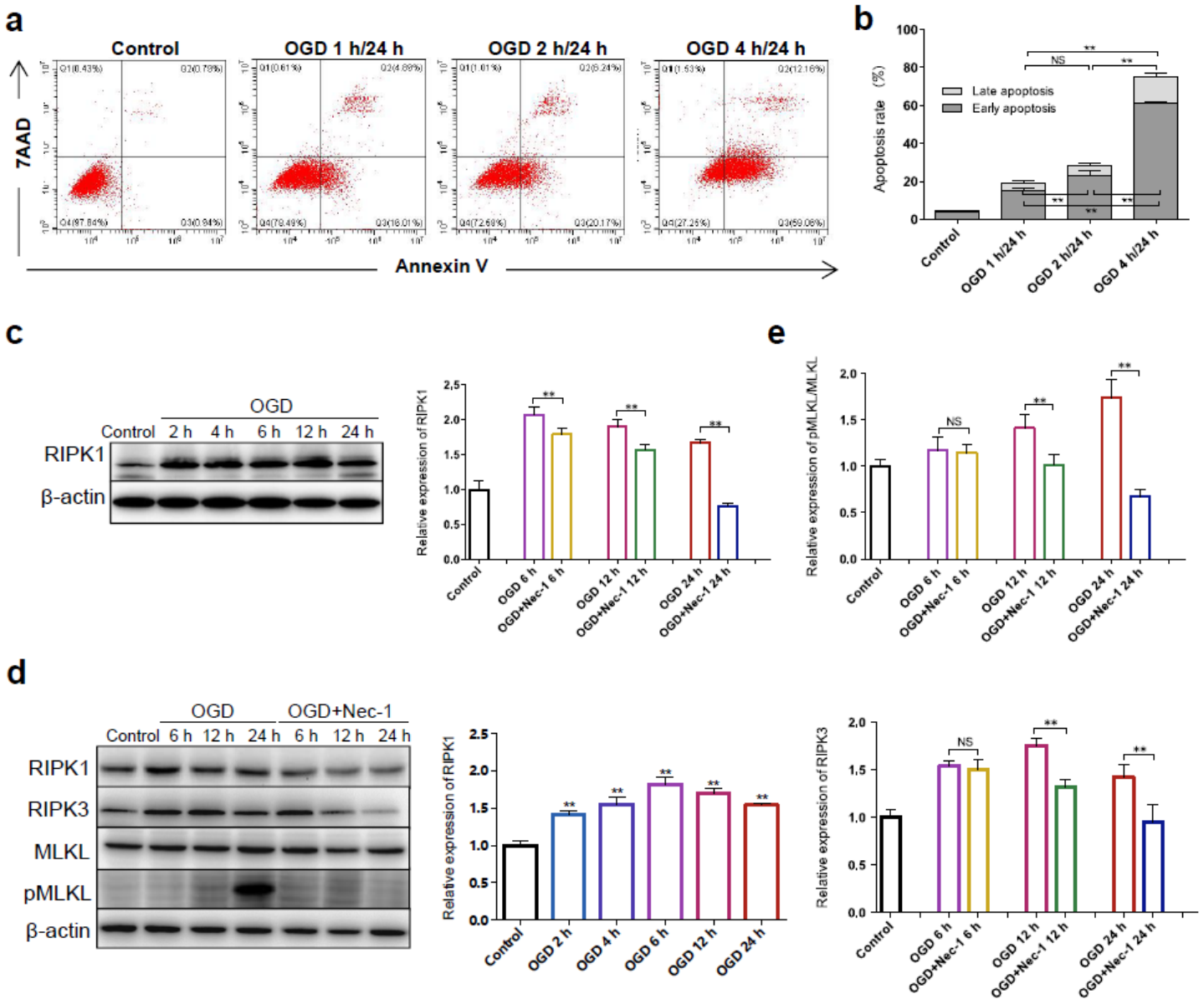

Figure 2

Nec-1 treatment lessened necroptosis of OGD microglia in vitro. a Apoptosis rate of microglia at 1 h, 2 h and 4 h of OGD following 24 h reperfusion were detected by Flow cytometry using Annexin V/7AAD staining. b Quantification analysis of Flow cytometry. c RIPK1 levels were analyzed at 4 h of OGD following 2 h, 4 h, 6 h, 12 h and 24 h reperfusion by western blot. d Necroptosis protein levels with Nec-1 treatment at 4 h of OGD following reperfusion were examined by using Western blot. Quantification data of RIPK1, RIPK3, and e pMLKL/MLKL. **P<0.01; NS, no significance.

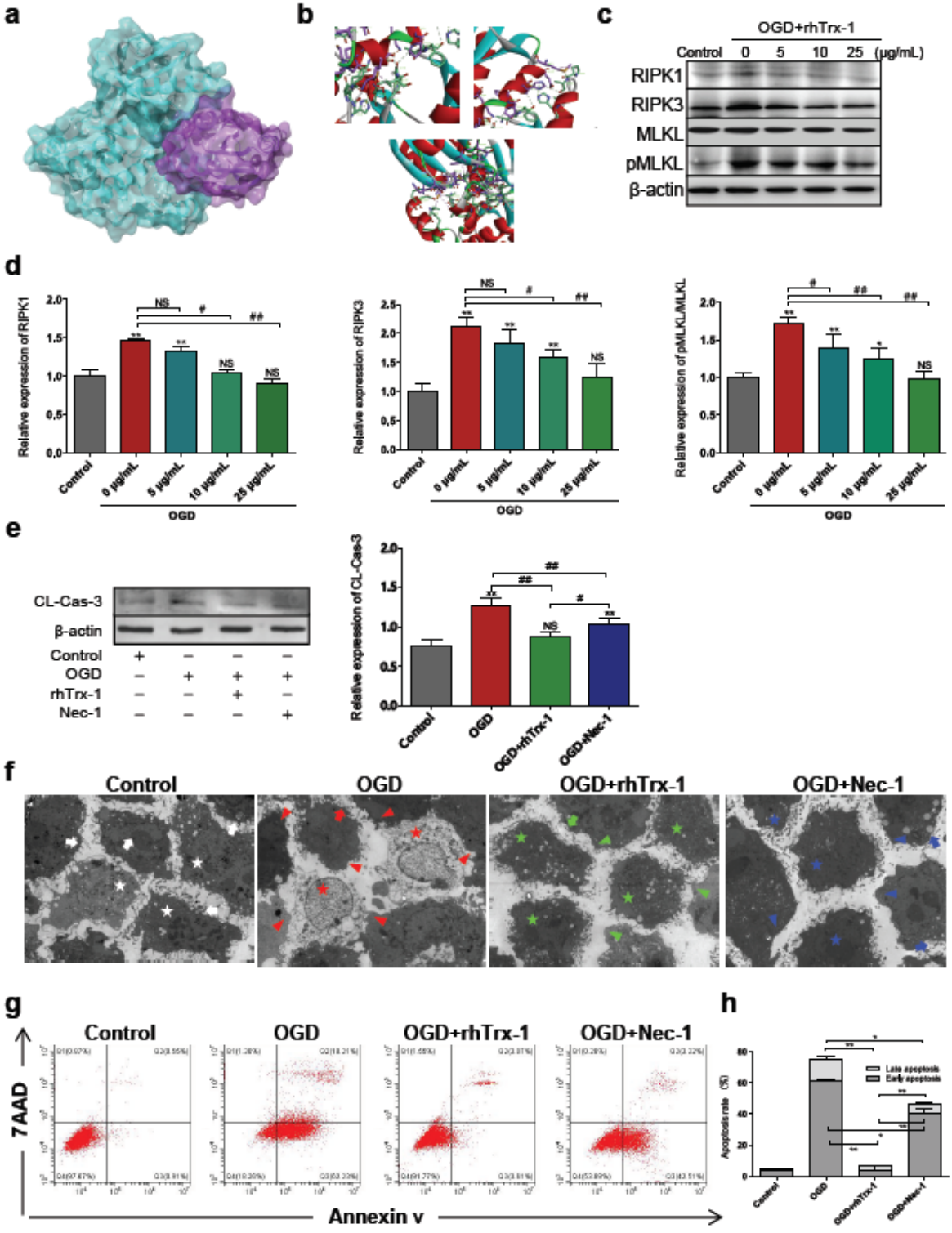

Figure 3

Effect of rhTrx-1 treatment on necroptosis and apoptosis in vitro. a Docking of RIPK1 and rhTrx-1. Green molecular represents RIPK1 and purple molecular represents rhTrx-1. b Interface Analysis of docking. c Representative images of the difference dose of rhTrx-1 treatment on the expression of necroptosis pathway proteins 24 h after OGD. d Quantification analysis of the protein levels of RIPK1, RIPK3, and pMLKL/MLKL. e Western blot analyis of CL-Cas-3 (Cleaved-Caspase-3) level and quantification data were

displayed. f Ultrastructural changes of rhTrx-1 and Nec-1 treatment cells (white, green and blue stars: normal cells; red stars: necrotic cells; Arrows: microvilli on the surface of cell membrane; Triangle: blebbing , 1000 X). g Annexin V/7AAD double-staining images of rhTrx-1 and Nec-1 treatment cells. h Quantification analysis of Annexin V/7AAD. *P<0.05, **P<0.01; #P<0.05, ##P<0.01; NS, no significance.

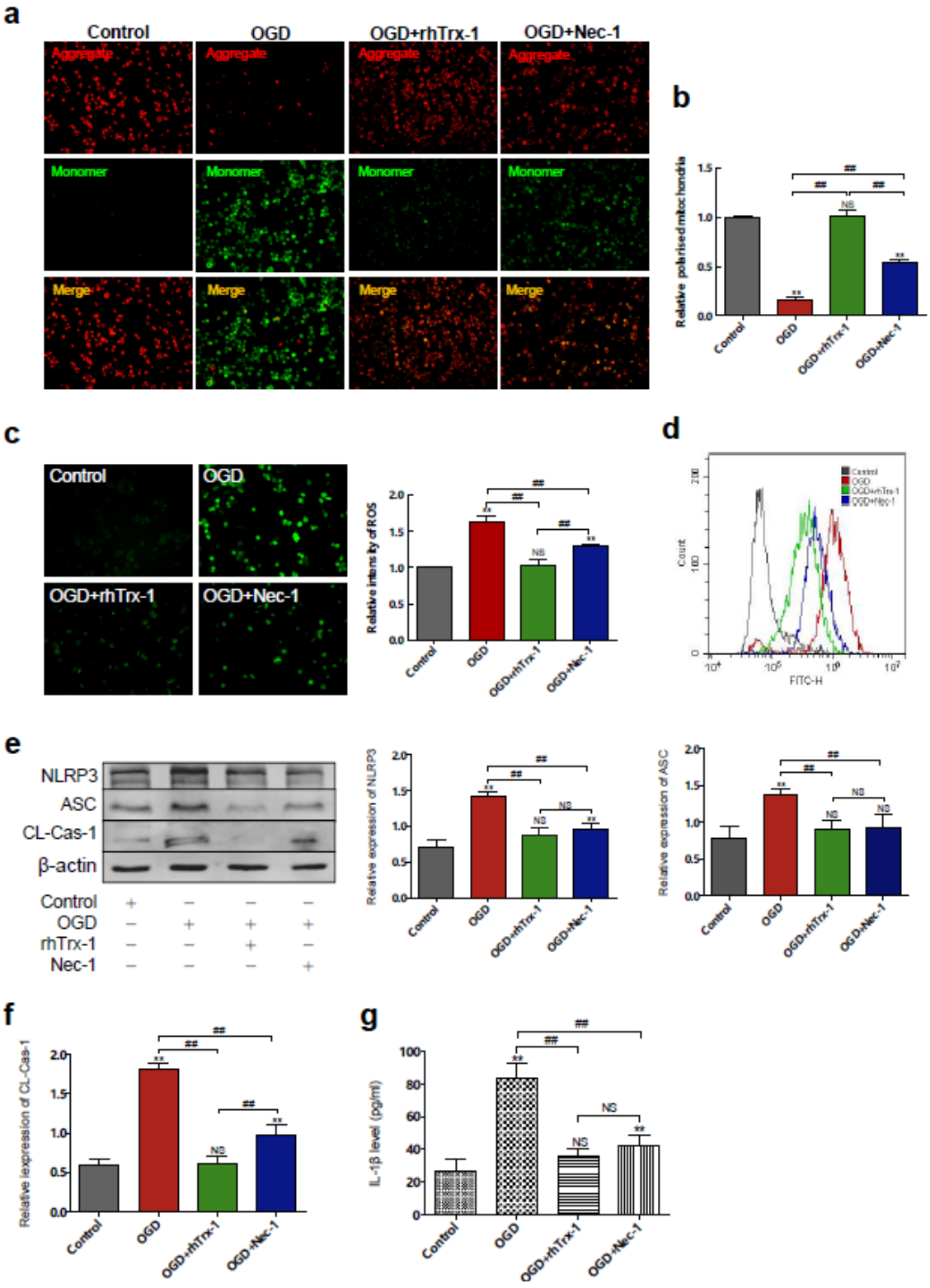

Figure 4

Measurement of mitochondrial membrane potential, ROS and NLRP3 inflammasome activation. a JC-1 staining was detected using fluorescence staining. b Relative ratio of aggregate to monomer was analyzed. c Fluorescence intensity of ROS was analyzed by using fluorescence staining and d Flow cytometry. e Western blot Images of NLRP3 inflammasome and quantitive analysis of NLRP3, ASC and f CL-Cas-1 (Cleaved-Caspase-1) levels. g ELISA data of IL-1β. Scale bar represents 50 μm. **P<0.01; ##P<0.01; NS, no significance.

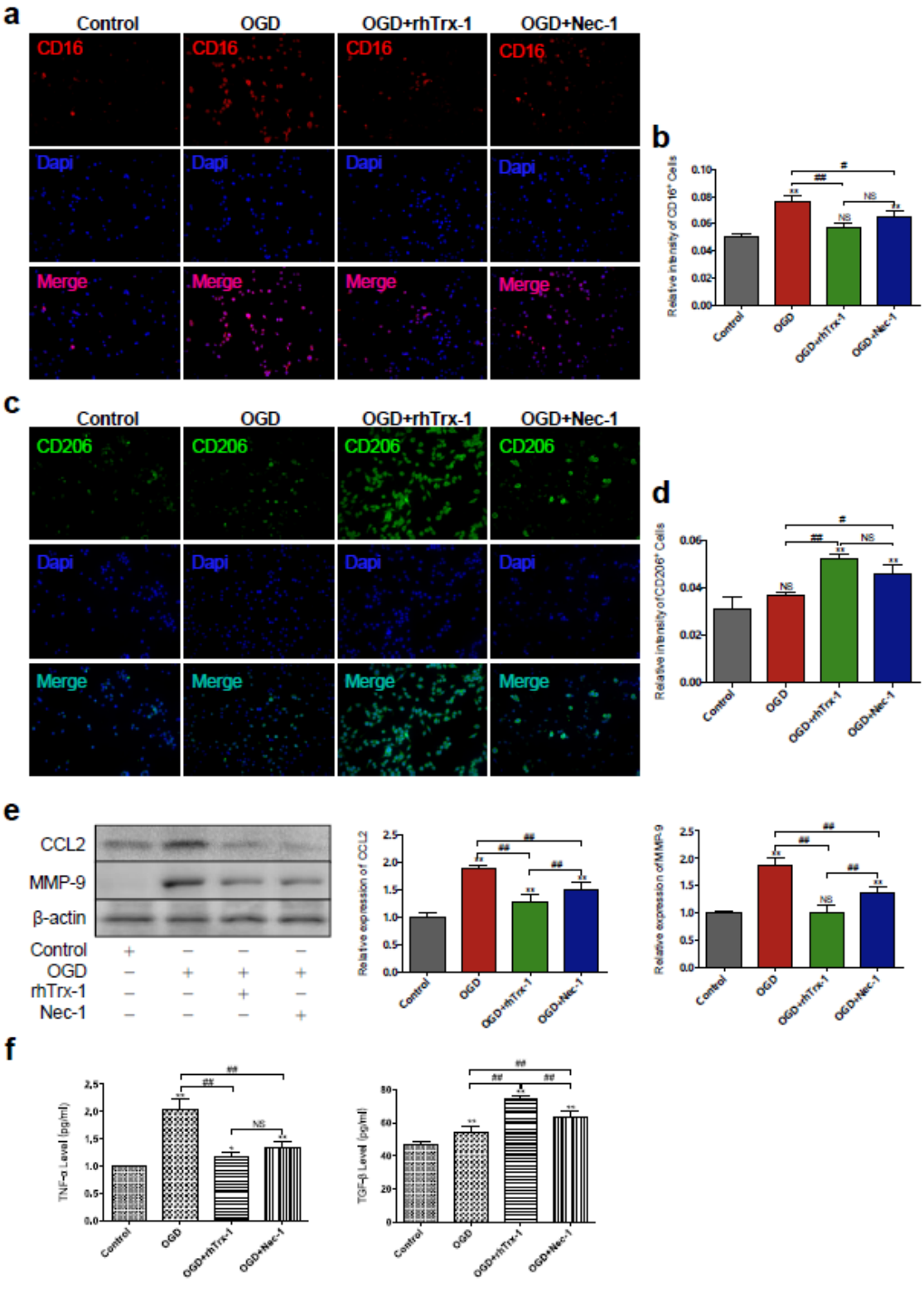

Figure 5

Therapeutic effect with rhTrx-1 regulated OGD-induced microglia polarization and inhibited the release of inflammation mediators. a Fluorescence staining of CD16 and Dapi. b Quantification analysis of the fluorescence intensity of CD16+ cells. c Fluorescence staining of CD206 and Dapi. d Quantification analysis of the fluorescence intensity of CD206+ cells. e Western blot analysis of CCL2 and MMP-9 levels. f ELISA data of TNF-α and TFG-β. Scale bar represents 50 μm. *P<0.05, **P<0.01; #P<0.05, ##P<0.01; NS, no significance.

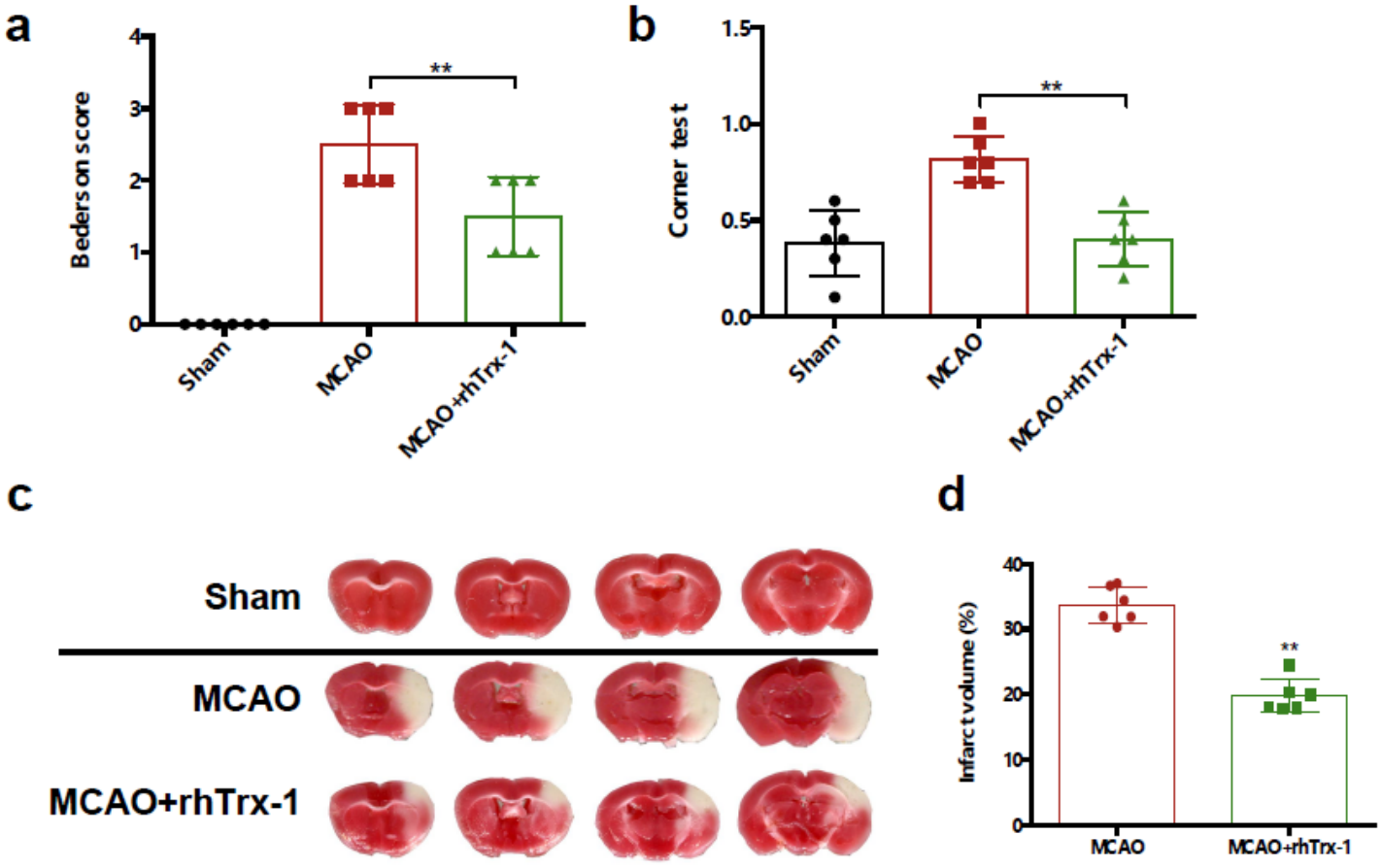

Figure 6

Investigation of neurological function and cerebral infarction. a Quantification analysis of bederson score. b Quantification analysis of Corner test. c TTC staining of mice brain. d Quantification analysis ofTTC staining. **P<0.01; ##P<0.01; NS, no significance.

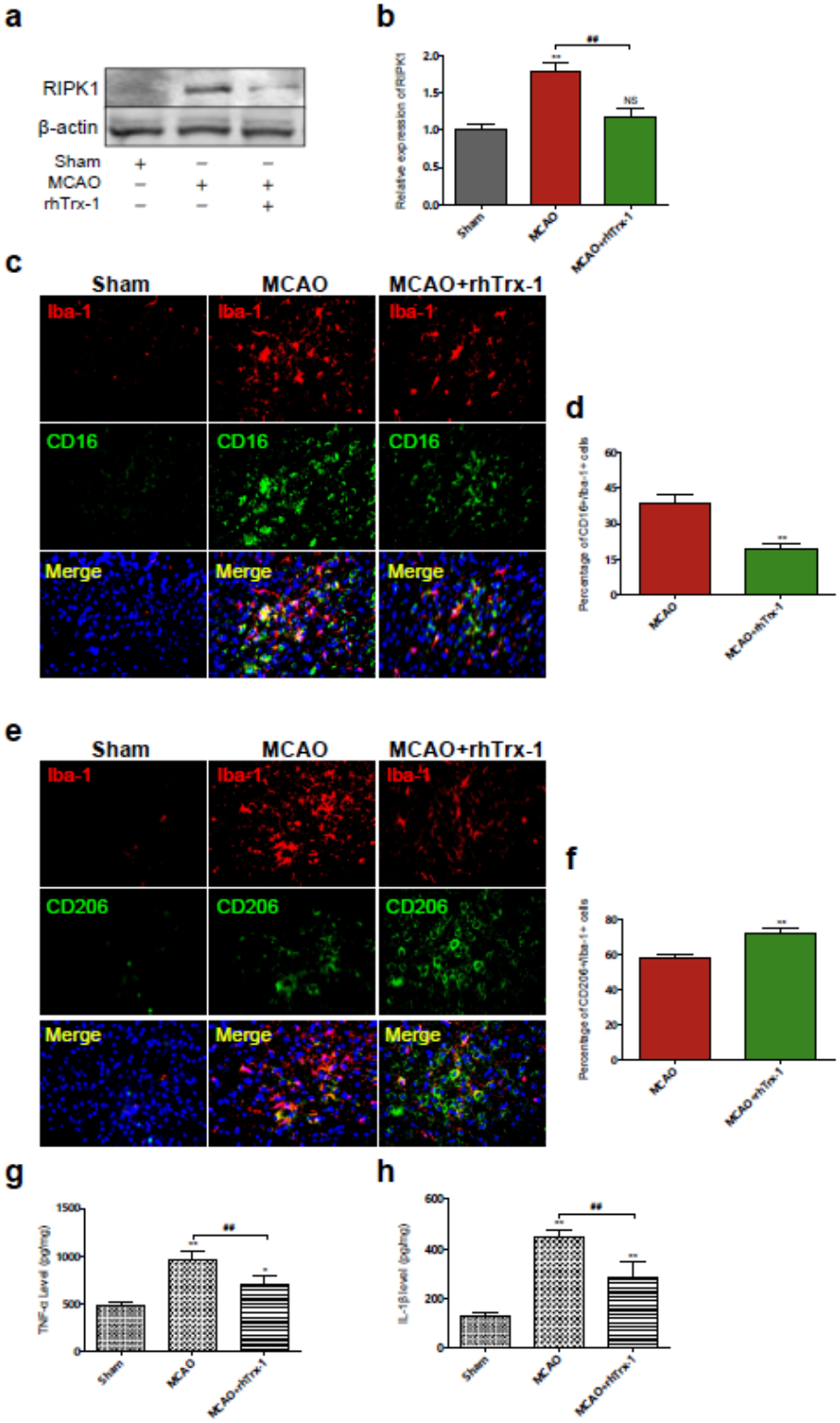

Figure 7

Detection of RIPK1 level, microglia polarization and inflammation factors in MCAO mice. a RIPK1 level was detected using western blot in the MCAO with the administration of rhTrx-1. b Quantification analysis of RIPK1 level. c Fluorescence staining of Iba-1, CD16 and Dapi. d Quantification data of CD16+ cell number. e Fluorescence staining of Iba-1, CD206 and Dapi. f Quantification data of CD206+ cell number.

g ELISA data of TNF-α. h ELISA data of IL-1β. Scale bar represents 50 μm. *P<0.05, **P<0.01; ##P<0.01; NS, no significance.

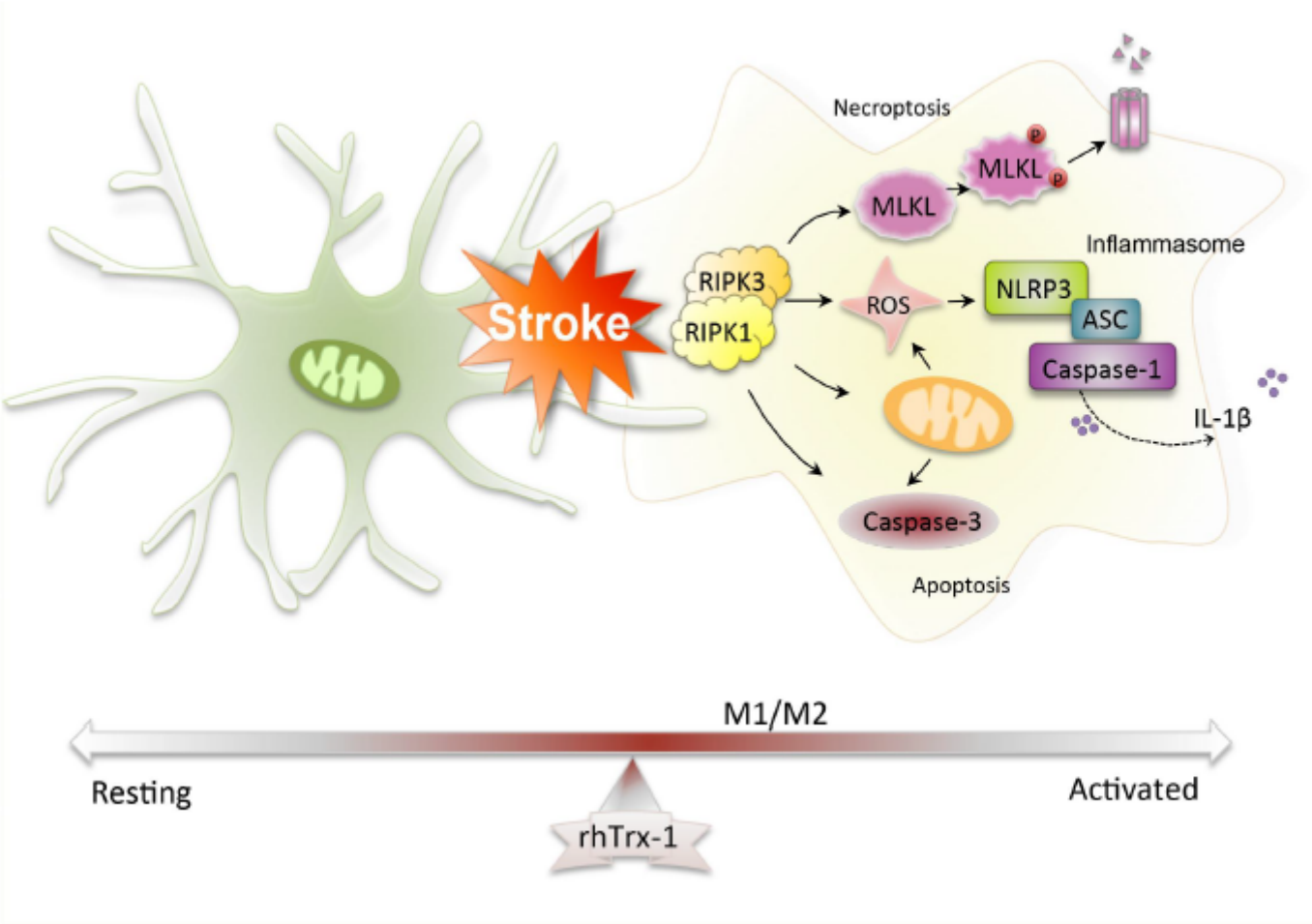

Figure 8

Mechanisms of rhTrx-1 treatment on cerebral ischemic stroke-induced microglia activation involved RIPK1-mediated necroptosis, apoptosis and NLRP3 inflammasome.

Supplementary Files

This is a list of supplementary files associated with this preprint. Click to download.

- Additionalfile1InterfaceAnalysis.xlsx